Springer

KSME

Journal of Mechanical Science and Technology 26 (11) (2012) 3399~3410
www.springerlink.com/content/1738-494x
DOI 10.1007/s12206-012-0860-2

Free vibration analysis of multi-directional functionally graded circular and annular plates †

Iman Davoodi Kermani, Mostafa Ghayour and Hamid Reza Mirdamadi*

Department of Mechanical Engineering, Isfahan University of Technology, Isfahan 84156-83111, Iran

(Manuscript Received December 27, 2011; Revised May 5, 2012; Accepted June 5, 2012)

Abstract

This paper addresses the free vibration of multi-directional functionally graded circular and annular plates using a semi-analytical/numerical method, called state space-based differential quadrature method. Three-dimensional elasticity equations are derived for multi-directional functionally graded plates and a solution is given by the semi-analytical/numerical method. This method gives an analytical solution along the thickness direction, using a state space method and a numerical solution using differential quadrature method. Some numerical examples are presented to show the accuracy and convergence of the method. The most of simulations of the present study have been validated by the existing literature. The non-dimensional frequencies and corresponding displacements mode shapes are obtained. Then the influences of thickness ratio and graded indexes are demonstrated on the non-dimensional natural frequencies.

Keywords: Circular plates; Differential quadrature method; Free vibration; Functionally graded materials (FGM); Multi-directional; State space-based formulation

1. Introduction

The concept of functionally graded materials (FGMs) was first introduced in 1984 as ultrahigh-temperature-resistant materials for aircraft, space vehicles and other engineering applications. FGMs are composite materials that are microscopically inhomogeneous, and their mechanical properties vary continuously in one or more directions. This is achieved by gradually varying the volume fraction of the constituent materials. The continuity of the material properties reduces the influence of the presence of abrupt interfaces and avoids high interfacial stresses. Furthermore, functionally graded materials can be designed to achieve particular desired properties and the gradation in properties of material can optimize the stress distribution.

By an increasing attention to FGMs, many researches have been done about these materials. For example, Prakash and Ganapathi [1] analyzed the asymmetric flexural vibration and thermoelastic stability of FGM circular plates. They used a finite element method to solve the problem. Efraim and Eisenberger [2] studied the exact vibration analysis of variable thickness thick annular isotropic and FGM plates. The motion equations which they obtained by first order shear deformation theory was solved by exact element method. Dong [3] presented analysis of three-dimensional free vibration of functionally graded annular plates via Chebyshev-Ritz method. Allahverdizadeh et al. [4] discussed the nonlinear free and forced vibration of thin annular plates which made of functionally graded material. They used assumed-time mode method and Kantorovich time averaging technique to solve the axisymmetric vibration problem. Nie and Zhong [5] studied the vibration of a sectorial annular FGM plate with simply supported radial edges. Analytical investigation on axisymmetric free vibrations of moderately thick circular functionally graded plate integrated with piezoelectric layers was presented by Rastgoo [6]. Malekzadeh et al. [7] analyzed the in-plane free vibration of functionally graded circular arches with temperature-dependent properties under thermal environment. They assumed that the material properties and temperature vary along thickness direction, the government equation and boundary conditions were obtained by Hamilton principle. Ebrahimi [8] studied geometrically nonlinear vibration of piezoelectrically actuated FGM plate with an initial large deformation, based on Kirchhoff's-Love hypothesis with von-Karman type geometrical large nonlinear deformation. Ghorbanpour Arani et al. [9] obtained a semi-analytical solution of magneto-thermo-elastic stresses for functionally graded variable thickness rotating disks. Malekzadeh et al. [10] analyzed the three-dimensional free vibration of thick functionally graded annular plates in thermal environment. They used the three-dimensional thermoelastic equilibrium equations and Hamilton principle to derive the motion equations. A novel

*Corresponding author. Tel.: +989133163147, Fax.: +983113912628
E-mail address: hrmirdamadi@cc.iut.ac.ir
† Recommended by Associate Editor Cheolung Cheong

approach for in-plane/out-of-plane frequency analysis of functionally graded circular/annular plates was obtained by Hosseini et al. [11]. Second-order shear deformation theory was employed to analyze vibration of temperature-dependent solar functionally graded plates by Shahrjerdi et al. [12]. Hao et al. [13] discussed the nonlinear dynamic response of a simply supported rectangular functionally graded material plate under the time-dependent thermal mechanical loads.

In the above-mentioned papers, material properties were variable in one-direction. Fabrication of engineering components with variable properties in two or more directions is a novel idea of using FGMs. Qian and Batra [14] designed bi-directional functionally graded rectangular plate for optimal natural frequencies. Axisymmetric bending of two-directional functionally graded circular and annular plates was studied by Nie and Zhong [15]. Lu et al. [16] obtained a semi-analytical solution for bi-directional functionally graded beams. Elastic-plastic analysis of two-dimensional functionally graded materials under thermal loading was presented by Nemat-alla et al. [17]. Lu et al. [18] analyzed 3-D elasticity problem for multi-directional functionally graded rectangular plates. Nie and Zhong [19] achieved dynamic analysis of multi-directional functionally graded annular plates using the state space-based differential quadrature method. Sobhani Aragh et al. [20] considered a novel 2-D parameter power-low distribution and investigated free vibration and vibrational displacements of two-dimensional functionally graded fiber-reinforced curved panels.

The differential quadrature method is a numerical technique that is used in some of the above-mentioned papers. This recent method was extensively used in vibration analysis, for example, Liew and Liu [21] presented the vibration analysis of shear deformable annular sectorial plates by differential quadrature method. Kitipornchai et al. [22] used a combination of differential quadrature method, Galerkin technique, and an iteration process to solve the nonlinear vibration of laminated FGM plates with geometric imperfections. Three-dimensional free vibration of inhomogeneous thick orthotropic shells of revolution using differential quadrature was studied by Redekop [23]. Kang [24], used differential quadrature method to solve the vibration analysis of thin-walled curved beams. Krowiak [25] presented the methods based on the differential quadrature and their application to the free vibration analysis of plates. Tornabene [26] studied free vibration analysis of functionally graded conical, cylindrical, shell, and annular plate structures with a four-parameter power-law distribution. He used generalized differential quadrature method to solve the motion equations which were obtained via first-order shear deformation theory (FSDT), and linear elasticity theory. In another work Tornabene et al. [27] obtained a 2-D differential quadrature solution for vibration analysis of functionally graded conical, cylindrical, shell, and annular plate structures. Hosseini et al. [28] studied vibration of radially FGM sectorial plates of variable thickness on elastic foundation; the solution of this problem was obtained by differential quadrature method.

In the present paper, the state space based differential quadrature method is used to analyze the free vibration problem. This method is a semi-analytical method which uses analytical state space method to solve problem in one direction, and numerical differential quadrature method to obtain the solution in another direction. This solution procedure was commonly used in vibration problems and some of them were mentioned previously. Furthermore, Chen et al. [29] used state space based differential quadrature method to present free vibration analysis of generally laminated beams. Nie and Zhong [30] used a semi-analytical state space based differential quadrature method for three-dimensional vibration analysis of circular FGM plates. Free vibration of a functionally graded piezoelectric beam via state space based differential quadrature was discussed by Yang and Zhifei [31]. Three-dimensional analysis of functionally graded annular plates using state space based differential quadrature method and comparative behavior modeling by artificial neural network investigated by Jodaei et al. [32].

Our contribution in this research is analyzing the free vibrations of circular and annular plates that are made of multi-directional functionally graded materials. In the above-mentioned papers, except [19], the material properties, in vibration problem of circular and annular plates, varied only in the thickness direction. In this paper, like Nie and Zhong's work [19], the material properties are variable in both radial and thickness directions. The difference between this work and Ref. [19] is in geometry and boundary conditions of plate. In addition, we demonstrate the influence of different parameters on natural frequencies and determine the corresponding mode shapes. We obtain the natural frequencies of free vibration of multi-directional functionally graded circular and annular plates by the state space-based differential quadrature method.

The remainder of the paper is organized as follows: In section 2, the equations of motion for a multi-directional functionally grade circular plate is obtained. In section 3, the differential quadrature method is used in radial direction and the equations are solved analytically in thickness direction by the state space method. In section 4, the numerical results are presented and the influences of different parameters on the natural frequencies of the plate are demonstrated. In section 5, the conclusions of the numerical results are discussed.

2. Basic formulation

Consider an isotropic annular plate with outer radius a, inner radius b and thickness h, as shown in Fig. 1. A cylindrical coordinate system (r, θ, z) with the origin O at the center of the bottom surface is employed to describe the plate geometry and displacements.

The 3D equations of motion in cylindrical polar coordinates, in the absence of body forces, are [19]:

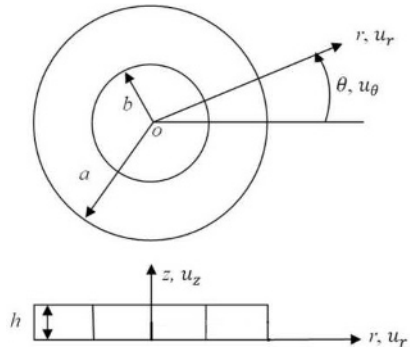

Fig. 1. A functionally graded annular plate.

$$\begin{aligned}
&\frac{\partial \sigma_r}{\partial r}+\frac{1}{r}\frac{\partial \tau_{r\theta}}{\partial \theta}+\frac{\partial \tau_{rz}}{\partial z}+\frac{\sigma_r-\sigma_\theta}{r}=\rho\frac{\partial^2 u_r}{\partial t^2},\\
&\frac{\partial \tau_{r\theta}}{\partial r}+\frac{1}{r}\frac{\partial \sigma_\theta}{\partial \theta}+\frac{\partial \tau_{\theta z}}{\partial z}+\frac{2\tau_{r\theta}}{r}=\rho\frac{\partial^2 u_\theta}{\partial t^2},\\
&\frac{\partial \tau_{rz}}{\partial r}+\frac{1}{r}\frac{\partial \tau_{\theta z}}{\partial \theta}+\frac{\partial \sigma_{rz}}{\partial z}+\frac{\tau_{rz}}{r}=\rho\frac{\partial^2 u_z}{\partial t^2}.
\end{aligned} \tag{1}$$

The constitutive equations for a linear, isotropic, functionally graded material can be written as [30]:

$$\begin{aligned}
&\sigma_r=C_{11}\varepsilon_r+C_{12}\varepsilon_\theta+C_{13}\varepsilon_z, \qquad \tau_{\theta z}=C_{44}\gamma_{\theta z},\\
&\sigma_\theta=C_{21}\varepsilon_r+C_{22}\varepsilon_\theta+C_{23}\varepsilon_z, \qquad \tau_{rz}=C_{55}\gamma_{rz},\\
&\sigma_z=C_{31}\varepsilon_r+C_{32}\varepsilon_\theta+C_{33}\varepsilon_z, \qquad \tau_{r\theta}=C_{66}\gamma_{r\theta}.
\end{aligned} \tag{2}$$

The C_{ij}^0 are the elastic stiffness components [3]:

$$\begin{aligned}
&\varepsilon_r=\frac{\partial u_r}{\partial r}, \qquad &&\gamma_{\theta z}=\frac{1}{r}\frac{\partial u_z}{\partial \theta}+\frac{\partial u_\theta}{\partial z},\\
&\varepsilon_\theta=\frac{1}{r}\frac{\partial u_\theta}{\partial \theta}+\frac{u_r}{r}, \qquad &&\gamma_{rz}=\frac{\partial u_r}{\partial z}+\frac{\partial u_z}{\partial r},\\
&\varepsilon_z=\frac{\partial u_z}{\partial z}, \qquad &&\gamma_{r\theta}=\frac{\partial u_\theta}{\partial r}+\frac{1}{r}\frac{\partial u_r}{\partial \theta}-\frac{u_\theta}{r}.
\end{aligned} \tag{3}$$

The 3D linearized strain-displacement relations are [30]:

$$\left[C^0\right]=\frac{E^0(1-\upsilon)}{(1+\upsilon)(1-2\upsilon)}\begin{bmatrix}
1 & C_1 & C_1 & 0 & 0 & 0\\
C_1 & 1 & C_1 & 0 & 0 & 0\\
C_1 & C_1 & 1 & 0 & 0 & 0\\
0 & 0 & 0 & C_2 & 0 & 0\\
0 & 0 & 0 & 0 & C_2 & 0\\
0 & 0 & 0 & 0 & 0 & C_2
\end{bmatrix}, \tag{4}$$

$$C_1=\frac{\upsilon}{1-\upsilon}, \quad C_2=\frac{1-2\upsilon}{2(1-\upsilon)}.$$

In FGMs, the material properties are a function of coordinates (r, θ, z) and vary continuously in one or more directions. In multi-directional functionally graded materials, the properties are variable in more than one direction. In the present paper, we assume that the material properties have the following exponential distributions in the thickness and radial directions of the plate [19]:

$$C_{ij}(r,z)=C_{ij}^0(0,0)e^{\lambda_1\left(\frac{z}{h}\right)+\lambda_2\left(\frac{r}{a}\right)} \tag{5a}$$

$$\rho(r,z)=\rho^0(0,0)e^{\lambda_1\left(\frac{z}{h}\right)+\lambda_2\left(\frac{r}{a}\right)}. \tag{5b}$$

Delale and Erdogan [33] indicated that the effect of Poisson's ratio on the deformation is much less than that of Young's modulus. Thus, Poisson's ratio of the plate is assumed to be constant. Substituting Eqs. (2)-(5) in Eq. (1), the dynamic equilibrium equations can be written in a state space form [19]:

$$\frac{\partial}{\partial z}\begin{bmatrix}\Pi\\ \Gamma\end{bmatrix}=\begin{bmatrix}0 & I\\ B_1 & B_2\end{bmatrix}\begin{bmatrix}\Pi\\ \Gamma\end{bmatrix}. \tag{6}$$

For an annular plate, the kinematic boundary conditions at inner edge ($r = b$) and outer edge ($r = a$) are expressed as follow [19]:

Clamped:

$$at\ r=b\ or\ r=a:\ u_r=0,\ u_\theta=0,\ u_z=0. \tag{7}$$

Simply supported:

$$at\ r=b\ or\ r=a:\ \sigma_r=0,\ u_\theta=0,\ u_z=0. \tag{8}$$

Free:

$$at\ r=b\ or\ r=a:\ \sigma_r=0,\ \tau_{r\theta}=0,\ \tau_{rz}=0. \tag{9}$$

For a solid circular plate the edge boundary condition is one of the above equations and the regularity conditions on the central point are [30]:

$$at\ r=0:\ u_r=0,\ u_\theta=0,\ \frac{\partial u_z}{\partial r}=0. \tag{10}$$

For free vibration problems, the stress boundary conditions at the bottom and top plate surfaces are assumed as the following [19]:

$$at\ z=0:\ \tau_{rz}=0,\ \tau_{\theta z}=0,\ \sigma_z=0 \tag{11}$$

$$at\ z=h:\ \tau_{rz}=0,\ \tau_{\theta z}=0,\ \sigma_z=0. \tag{12}$$

3. Solution

Obtaining an analytical solution for the state space formulation (6) is difficult. Thus, a semi-analytical solution is used to analyze the free vibration of multi-direction functionally graded circular and annular plates, which gives an analytical

solution in thickness direction and a numerical solution in radial direction. The analytical solution in the thickness direction is obtained by the state space description and the one-dimensional differential quadrature method is used to obtain a numerical solution in the radial direction of the plate. When a circular or annular plate is vibrating with natural frequency ω, the displacement field can be assumed as follows [19]:

$$\begin{aligned} u_r(r,\theta,z,t) &= \tilde{u}_r(r,z)\cos(m\theta)e^{i\omega t}, \\ u_\theta(r,\theta,z,t) &= \tilde{u}_\theta(r,z)\sin(m\theta)e^{i\omega t}, \\ u_z(r,\theta,z,t) &= \tilde{u}_z(r,z)\cos(m\theta)e^{i\omega t}. \end{aligned} \tag{13}$$

By introducing the following non-dimensional parameters [19]:

$$\begin{aligned} &Z=\frac{z}{h}, \quad R=\frac{r}{a}, \quad U_R=\frac{\tilde{u}_r}{h}, \quad U_\theta=\frac{\tilde{u}_\theta}{h}, \quad U_Z=\frac{\tilde{u}_Z}{h}, \\ &\bar{C}_{ij}^0=\frac{C_{ij}^0}{C_{11}^0}, \quad \Omega=\omega h\sqrt{\frac{\rho^0}{C_{11}^0}}. \end{aligned} \tag{14}$$

Substituting Eq. (13) into Eq. (6), the state space equations can be given as [19]:

$$\frac{\partial}{\partial Z}\begin{bmatrix}\bar{\Pi}\\ \bar{\Gamma}\end{bmatrix}=\begin{bmatrix}0 & I\\ \bar{B}_1 & \bar{B}_2\end{bmatrix}\begin{bmatrix}\bar{\Pi}\\ \bar{\Gamma}\end{bmatrix}. \tag{15}$$

By applying the one-dimensional differential quadrature Method in the radial direction, the solution of the state space Eq. (15) will be obtained. The differential quadrature Method is a numerical method which divides the continuous solution domain into a set of finite points and replaces the derivatives of an arbitrary unknown function with the weighted summation of the functions values in the discretized points. The differential quadrature rule for *n*th-order derivative of a function *f(R)*, at point *i* can be expressed as follows [34]:

$$\left.\frac{d^n f(R)}{dR^n}\right|_{R=R_i}=\sum_{j=1}^{N}W_{ij}^{(n)}f(R_j) \qquad i=1,2,...,N. \tag{16}$$

There are different ways for calculating the weighting coefficient matrix, because different functions may be used as test functions. For polynomial basis functions used in DQM, a set of Lagrange polynomials are employed as the test functions; thus, the weighting coefficients for the first-order derivatives in the R-direction are thus determined as:

$$W_{ij}^{(1)}=\begin{cases}\dfrac{1}{a}\dfrac{M(R_i)}{(R_i-R_j)M(R_j)} & i\neq j\\ -\displaystyle\sum_{\substack{j=1\\ i\neq j}}^{N}W_{ij}^{(1)} & i=j\end{cases} \qquad i=1,2,...,N. \tag{17}$$

The weighting coefficients of the higher-order derivatives can be obtained as [34]:

$$\left[W^{(n)}\right]=\left[W^{(1)}\right]^n. \tag{18}$$

A usual choice of the point grid distribution is a uniform grid spacing rule. It was found that non-uniform grid spacing yields better accuracy. In this study, the Chebyshev-Gauss-Lobatto quadrature points are used [34]:

$$R_i=0.5\left[1-\cos\left(\frac{(i-1)\pi}{N-1}\right)\right](a-b)+b \quad i=1,2,...,N. \tag{19}$$

Substituting Eq. (16) into Eq. (14), the state space equations can be written as [19]:

$$\frac{\partial}{\partial Z}\begin{bmatrix}\bar{\Pi}_i\\ \bar{\Gamma}_i\end{bmatrix}=B_i\begin{bmatrix}\bar{\Pi}_i\\ \bar{\Gamma}_i\end{bmatrix}=\begin{bmatrix}0 & I\\ (\bar{B}_i)_1 & (\bar{B}_i)_2\end{bmatrix}\begin{bmatrix}\bar{\Pi}_i\\ \bar{\Gamma}_i\end{bmatrix}. \tag{20}$$

The solution of Eq. (20) can be written as [35]:

$$\begin{bmatrix}\bar{\Pi}_i(Z)\\ \bar{\Gamma}_i(Z)\end{bmatrix}=e^{B_iZ}\begin{bmatrix}\bar{\Pi}_i(0)\\ \bar{\Gamma}_i(0)\end{bmatrix}. \tag{21}$$

$\bar{\Pi}_i(Z)$, $\bar{\Gamma}_i(Z)$, $\bar{\Pi}_i(0)$ and $\bar{\Gamma}_i(0)$ are the values of the state variables at arbitrary plane Z and the reference bottom plane $Z=0$, respectively. From Eq. (21), for the values of the state variables at the top plane, $Z=1$, we get [19]:

$$\begin{bmatrix}\bar{\Pi}_i(1)\\ \bar{\Gamma}_i(1)\end{bmatrix}=e^{B_i}\begin{bmatrix}\bar{\Pi}_i(0)\\ \bar{\Gamma}_i(0)\end{bmatrix}. \tag{22}$$

Rewriting the boundary conditions in a non-dimensional form and discretizing by DQM, we obtain the following form of the boundary conditions for the center, inner and outer edges of the plate [30]:

Clamped:

$$at \ R=R_1: U_{R1}=0, \ U_{\theta 1}=0, \ U_{Z1}=0 \tag{23}$$

$$at \ R=R_N: U_{RN}=0, \ U_{\theta N}=0, \ U_{ZN}=0. \tag{24}$$

Simply supported:

$$at \ R=R_1: \sigma_{R1}=0, \ U_{\theta 1}=0, \ U_{Z1}=0 \tag{25}$$

$$at \ R=R_N: \sigma_{RN}=0, \ U_{\theta N}=0, \ U_{ZN}=0. \tag{26}$$

Free:

$$at \ R=R_1: \sigma_{R1}=0, \ \tau_{R\theta 1}=0, \ \tau_{RZ1}=0 \tag{27}$$

$$at\ \ R = R_N:\ \sigma_{RN} = 0,\ \tau_{R\theta N} = 0,\ \tau_{RZN} = 0. \tag{28}$$

Regularity conditions:

$$R = 0:\ U_{R1} = 0,\ U_{\theta 1} = 0,\ U_{Z1} = -\sum_{j=2}^{N} \frac{W_{1j}^{(1)}}{W_{11}^{(1)}} U_{Zj}\ . \tag{29}$$

For the bottom and top plate surfaces, $Z = 0$ and $Z = 1$, the discretized boundary conditions can be expressed as follows:

$$\begin{aligned} &\left(\frac{\partial U_R}{\partial Z}\right)_i + \frac{h}{a}\sum_{j=1}^{N} W_{ij}^{(1)} U_{Zj} = 0, \\ &\left(\frac{\partial U_\theta}{\partial Z}\right)_i - \frac{mh}{aR_i} U_{Zi} = 0, \qquad i = 1, 2, ..., N \\ &\left(\frac{\partial U_Z}{\partial Z}\right)_i + \frac{h\bar{C}_{13}^0}{a\bar{C}_{33}^0}\left(\sum_{j=1}^{N} W_{ij}^{(1)} U_{Rj} + \frac{mU_{\theta i}}{R_i} + \frac{U_{Ri}}{R_i}\right) = 0\ . \end{aligned} \tag{30}$$

These equations can be written in a matrix form [19]:

$$\begin{bmatrix} \bar{\Gamma}_i(0) \\ \bar{\Gamma}_i(1) \end{bmatrix} = D \begin{bmatrix} \bar{\Pi}_i(0) \\ \bar{\Pi}_i(1) \end{bmatrix}. \tag{31}$$

Substituting Eq. (30) into Eq. (22), and applying the boundary conditions, Eqs. (23)-(28), a set of linear algebraic and homogeneous equations for the plate free vibrations can be obtained [19]:

$$B \begin{bmatrix} \bar{\Pi}_i'(0) \\ \bar{\Pi}_i'(1) \end{bmatrix} = 0\ . \tag{32}$$

The non-trivial solution of Eq. (32) is obtained by setting [19]:

$$\det(B) = 0. \tag{33}$$

Solving the above equations determines the non-dimensional natural frequencies for the free vibrations of the multi-directional functionally graded circular or annular plates.

4. Numerical results and discussion

4.1 Circular plate with clamped edge

A multi-directional functionally graded circular plate with the radius $a = 1$ and thickness $h = 0.2$ assumed. Material properties at the center of the bottom surface of the plate are $E^0 = 380\ GPa$, $\rho^0 = 3800\ kg/m^3$ and $\upsilon = 0.3$. These properties, except the Poisson's ratio, are assumed to have an exponential distribution in the thickness and radius of the plate. According to Eq. (5):

– If $\lambda_1 = \lambda_2 = 0$ the plate is homogenous.

– If $\lambda_1 \neq 0$ and $\lambda_2 = 0$ the material properties vary only in thickness direction.

– If $\lambda_1 = 0$ and $\lambda_2 \neq 0$ it is a plate with variable properties in radial direction.

– If $\lambda_1 \neq 0$ and $\lambda_2 \neq 0$ the plate's material is multi-directional functionally graded with exponential distribution in both thickness and radial directions.

Table 1. The comparison of the lowest five non-dimensional frequencies of the circular plate ($h/a = 0.2$ and $\lambda_1 = \lambda_2 = 0$).

m		Ω_1	Ω_2	Ω_3	Ω_4	Ω_5
0	Ref. [36]	0.097	0.320	0.410	0.603	0.693
	Present	0.097	0.320	0.410	0.603	0.693
1	Ref. [36]	0.192	0.393	0.454	0.594	0.755
	Present	0.191	0.390	0.453	0.593	0.755

Table 2. The comparison of the first five non-dimensional frequencies of the circular plate ($h/a = 0.2$, $\lambda_1 = 1$ and $\lambda_2 = 0$).

m	Ref. [30]	Present				
	Ω_1	Ω_2	Ω_3	Ω_4	Ω_5	Ω_1
0	0.096	0.095	0.314	0.410	0.593	0.693
1	0.186	0.187	0.390	0.445	0.593	0.746
2	0.277	0.280	0.553	0.569	0.738	0.882

Table 3. The lowest five non-dimensional frequencies of the clamped circular plate ($h/a = 0.2$, $\lambda_1 = 0$ and $\lambda_2 = 1$).

m	Ω_2	Ω_3	Ω_4	Ω_5	Ω_1
0	0.113	0.335	0.453	0.617	0.709
1	0.203	0.436	0.465	0.621	0.765
2	0.297	0.575	0.589	0.758	0.904

First, consider the plate is homogenous ($\lambda_1 = \lambda_2 = 0$), the lowest five non-dimensional frequencies for two different numbers of circumferential waves are demonstrated in Table 1, and the accuracy of results is validated with those of Ref. [36]. The state space-based differential quadrature method is used to solve the equations. In the numerical solution, 10 discrete points are used.

From Table 2, it can be found that the present results for the case of $\lambda_1 \neq 0$ and $\lambda_2 = 0$ are in a good agreement with those in Ref. [30]. Table 3 illustrates the lowest five non-dimensional frequencies for the free vibrations of the circular plate with variable properties in the radial direction only ($\lambda_1 = 0$ and $\lambda_2 \neq 0$).

The first five non-dimensional frequencies for different thickness-to-radius ratios are listed in Table 4. The convergence of the method for the first three natural frequencies of bi-directional functionally graded circular plate with clamped edge is shown in Fig. 2. The influence of the graded indices on the first three natural frequencies is demonstrated in Figs. 3 and 4.

Fig. 3 indicates that the natural frequency for the symmetric values of thickness graded index is equal, because when the

Table 4. The lowest five non-dimensional frequencies of the clamped circular plate ($\lambda_1 = \lambda_2 = 1$).

h/a	*m*	Ω_2	Ω_3	Ω_4	Ω_5	Ω_1
0.1	0	0.030	0.098	0.200	0.227	0.325
	1	0.056	0.144	0.218	0.259	0.311
	2	0.086	0.190	0.287	0.315	0.379
0.2	0	0.110	0.329	0.453	0.607	0.709
	1	0.199	0.436	0.457	0.621	0.752
	2	0.291	0.575	0.579	0.758	0.890
0.3	0	0.225	0.609	0.680	1.057	1.062
	1	0.386	0.654	0.816	0.932	1.284
	2	0.545	0.864	1.014	1.136	1.439
0.4	0	0.360	0.903	0.907	1.406	1.518
	1	0.590	0.876	1.181	1.245	1.819
	2	0.814	1.151	1.454	1.513	2.030
0.5	0	0.504	1.133	1.201	1.742	1.953
	1	0.800	1.095	1.545	1.557	2.036
	2	1.087	1.436	1.878	1.889	2.248

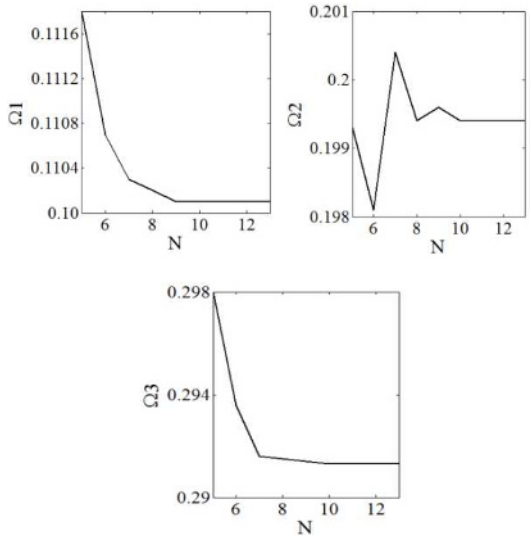

Fig. 2. The convergence of the first three natural frequencies ($h/a = 0.2$ and $\lambda_1 = \lambda_2 = 1$).

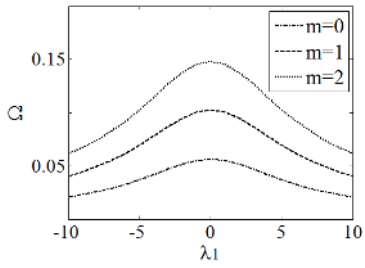

Fig. 3. The natural frequencies of circular clamped plate for different values of graded index in the thickness direction ($h/a = 0.2$ and $\lambda_2 = 1$).

sign of the thickness graded index changes is the same as the state in which the direction of z-axis changes. In addition,

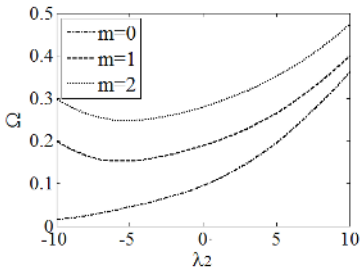

Fig. 4. The natural frequencies of circular clamped plate for different values of graded index in the radial direction ($h/a = 0.2$ and $\lambda_1 = 1$).

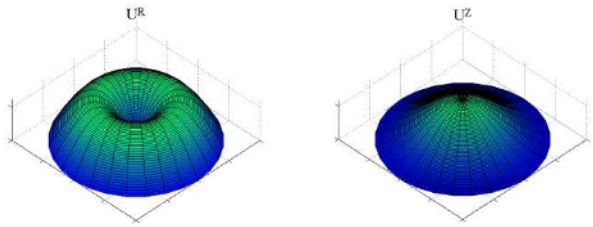

Fig. 5. Displacement mode shapes of a clamped circular plate corresponding to the first frequency of $m = 0$ ($h/a = 0.2$ and $\lambda_1 = \lambda_2 = 1$).

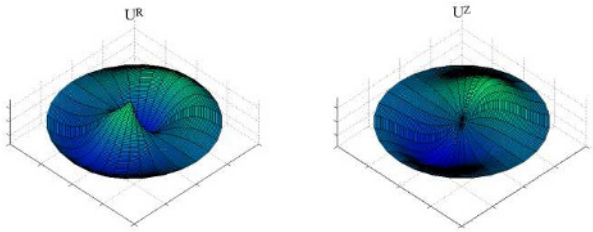

Fig. 6. Displacement mode shapes of a clamped circular plate corresponding to the first frequency of $m = 1$ ($h/a = 0.2$ and $\lambda_1 = \lambda_2 = 1$).

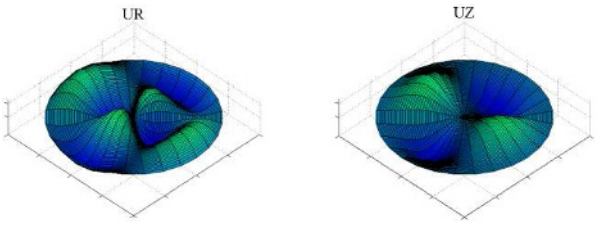

Fig. 7. Displacement mode shapes of a clamped circular plate corresponding to the first frequency of $m = 2$ ($h/a = 0.2$ and $\lambda_1 = \lambda_2 = 1$).

according to Fig. 3, when the absolute value graded index in thickness direction increases the natural frequencies of circular clamped plate decrease.

Fig. 4, shows that the natural frequencies of multi-directional functionally graded circular plate with clamped edge increase with an increase in radial graded index.

When the natural frequencies have been determined, the corresponding mode shapes can be evaluated by Eq. (32). The displacement mode shapes according to the first natural frequencies of circular clamped plate when, $m = 0$, 1, 2 are shown in Figs. 5-7, respectively. The nodal diameters are ob-

Table 5. The lowest three non-dimensional natural frequencies of a simply supported functionally graded circular plate (h/a = 0.1 and N = 12).

m	$\lambda_1=\lambda_2=1$	$\lambda_1=0,\lambda_2=1$	$\lambda_1=1,\lambda_2=0$	$\lambda_1=\lambda_2=0$
0	0.0121	0.0124	0.0120	0.0123
1	0.0361	0.0370	0.0356	0.0365
2	0.0624	0.0639	0.0622	0.0637

Table 6. The lowest five non-dimensional frequencies of the simply supported circular plate ($\lambda_1=\lambda_2=1$ and N = 8).

h/a	m	Ω_2	Ω_3	Ω_4	Ω_5	Ω_1
0.1	0	0.012	0.074	0.153	0.171	0.227
	1	0.036	0.064	0.116	0.231	0.310
	2	0.062	0.096	0.161	0.287	0.365
0.2	0	0.047	0.263	0.305	0.453	0.551
	1	0.132	0.135	0.393	0.620	0.675
	2	0.192	0.225	0.524	0.729	0.850
0.3	0	0.103	0.457	0.515	0.680	0.998
	1	0.208	0.271	0.738	0.930	0.978
	2	0.288	0.446	0.956	1.093	1.314
0.4	0	0.176	0.608	0.796	0.906	1.466
	1	0.290	0.436	1.104	1.244	1.293
	2	0.384	0.694	1.400	1.475	1.712
0.5	0	0.264	0.757	1.088	1.133	1.896
	1	0.366	0.614	1.473	1.556	1.589
	2	0.479	0.953	1.763	1.824	1.869

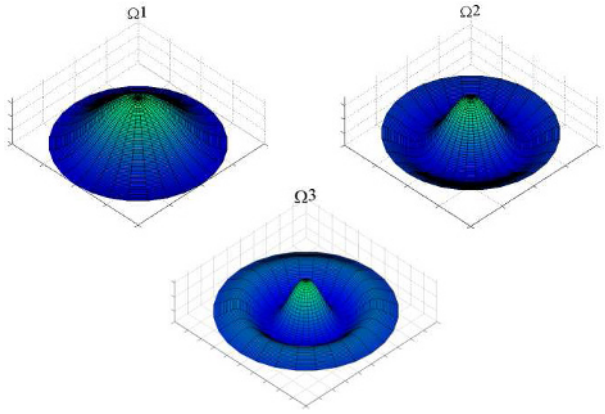

Fig. 8. Thickness displacement mode shapes of a clamped circular plate corresponding to the first three frequencies of m = 0 (h/a = 0.2 and $\lambda_1=\lambda_2=1$).

vious in these figures. The mode shapes of thickness displacement corresponding to the first three frequencies of circular clamped plate with zero wave number are demonstrated in Fig. 8.

4.2 Circular plate with simply supported edge

Consider a plate with the same properties as the plate of 4.1, which is simply supported. The lowest three non-dimensional natural frequencies of a simply supported circular plate for different kind of material distribution are listed in Table 5. According to Table 5, a plate with material property distribution in only radial direction has the largest natural frequencies. The lowest five dimensionless natural frequencies of simply supported bi-directional functionally graded circular plate for different thickness-to-radius ratios are presented in Table 6.

Figs. 9-11 show the displacements mode shape corresponding to the lowest natural frequencies of simply supported functionally graded circular plate.

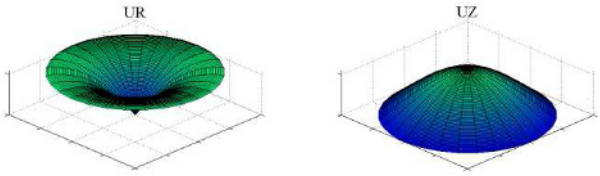

Fig. 9. Displacement mode shapes of the simply supported circular plate corresponding to the first frequency of m = 0 (h/a = 0.1 and $\lambda_1=\lambda_2=1$).

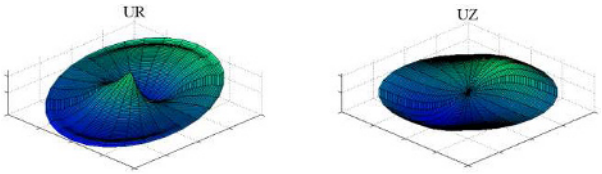

Fig. 10. Displacement mode shapes of the simply supported circular plate corresponding to the first frequency of m = 1 (h/a = 0.1 and $\lambda_1=\lambda_2=1$).

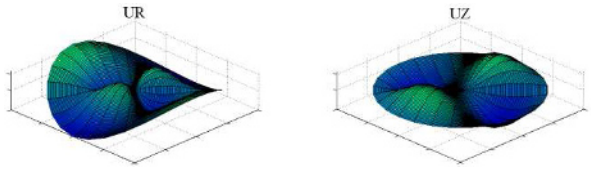

Fig. 11. Displacement mode shapes of the simply supported circular plate corresponding to the first frequency of m = 2 (h/a = 0.1 and $\lambda_1=\lambda_2=1$).

4.3 Annular plate with simply supported inner and clamped outer edges

Consider an annular plate with inner radius b, outer radius a, and thickness h; which its inner and outer edges are simply supported and clamped, respectively. The material properties of this plate are the same as plates were discussed in 4.1 and 4.2. The lowest three natural frequencies for four different case of graded material are presented in Table 7.

The lowest five dimensionless natural frequencies of bi-directional annular plate with simply supported inner and clamped outer edges via different inner radius-to-outer radius ratios and thickness-to-outer radius ratios are listed in Tables 8 and 9, respectively. Table 8, shows that the increase of the

Table 7. The lowest three non-dimensional natural frequencies of the functionally graded annular plate with simply supported inner and clamped outer edges (h/a = 0.2, b/a = 0.1 and N = 12).

m	$\lambda_1=\lambda_2=1$	$\lambda_1=0, \lambda_2=1$	$\lambda_1=1, \lambda_2=0$	$\lambda_1=\lambda_2=0$
0	0.195	0.199	0.189	0.193
1	0.219	0.223	0.209	0.213
2	0.294	0.299	0.283	0.288

Table 8. The lowest five non-dimensional frequencies of the annular plate with simply supported inner and clamped outer edges via different inner radius-to-outer radius ratios (h/a = 0.1, $\lambda_1=\lambda_2$ =1 and N = 10).

b/a	m	Ω_2	Ω_3	Ω_4	Ω_5	Ω_1
0.1	0	0.057	0.151	0.231	0.277	0.343
	1	0.064	0.161	0.241	0.289	0.330
	2	0.078	0.193	0.293	0.324	0.383
0.2	0	0.068	0.182	0.244	0.327	0.333
	1	0.074	0.189	0.261	0.339	0.340
	2	0.092	0.211	0.307	0.361	0.390
0.3	0	0.084	0.226	0.267	0.323	0.410
	1	0.089	0.231	0.286	0.340	0.414
	2	0.104	0.246	0.329	0.392	0.428

Table 9. The lowest five non-dimensional frequencies of the annular plate with simply supported inner and clamped outer edges via different thickness-to-outer radius ratios (b/a = 0.1, $\lambda_1=\lambda_2$ = 1 and N = 10).

h/a	m	Ω_2	Ω_3	Ω_4	Ω_5	Ω_1
0.1	0	0.057	0.151	0.231	0.277	0.343
	1	0.064	0.161	0.241	0.289	0.330
	2	0.078	0.193	0.293	0.324	0.383
0.2	0	0.196	0.462	0.463	0.687	0.785
	1	0.219	0.483	0.496	0.661	0.810
	2	0.294	0.585	0.587	0.765	0.906
0.3	0	0.368	0.693	0.811	1.031	1.215
	1	0.415	0.725	0.870	0.991	1.376
	2	0.548	0.878	1.022	1.146	1.520
0.4	0	0.552	0.924	1.162	1.373	1.620
	1	0.625	0.967	1.249	1.321	1.922
	2	0.817	1.170	1.464	1.527	2.057

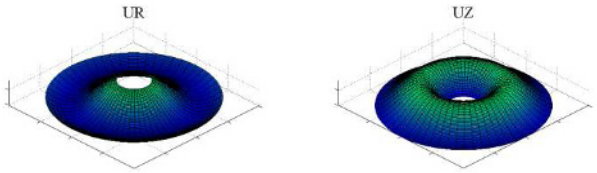

Fig. 12. Displacement mode shapes of the annular plate with simply supported inner and clamped outer edges corresponding to the first frequency of m = 0 (h/a = 0.1, b/a = 0.2 and $\lambda_1=\lambda_2$ = 1).

inner radius-to-outer radius ratio increases the natural frequencies of the annular functionally graded plate with simply supported inner and clamped outer edges. According to Table 9, the natural frequencies increase when the thickness-to-outer radius ratio increases.

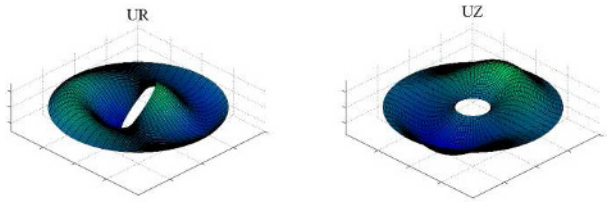

Fig. 13. Displacement mode shapes of the annular plate with simply supported inner and clamped outer edges corresponding to the first frequency of m = 1 (h/a = 0.1, b/a = 0.2 and $\lambda_1=\lambda_2$ = 1).

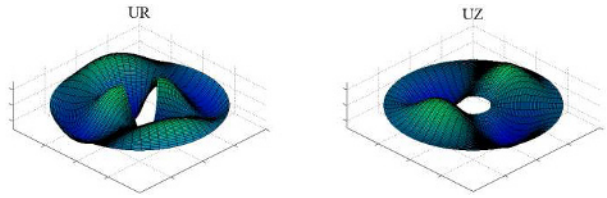

Fig. 14. Displacement mode shapes of the annular plate with simply supported inner and clamped outer edges corresponding to the first frequency of m = 2 (h/a = 0.1, b/a = 0.2 and $\lambda_1=\lambda_2$ = 1).

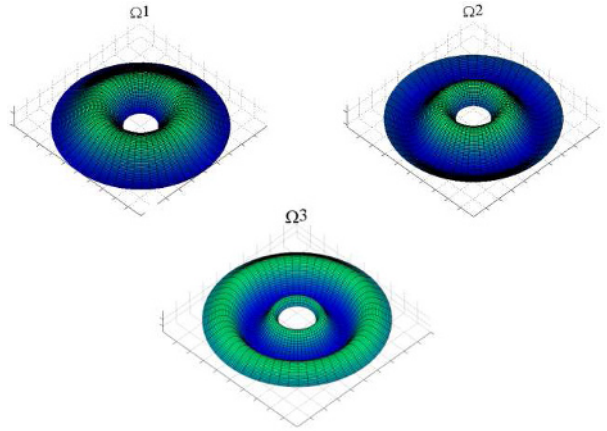

Fig. 15. Thickness displacement mode shapes of the annular plate with simply supported inner and clamped outer edges plate corresponding to the first three frequencies of m = 0 (h/a = 0.1, b/a = 0.2 and $\lambda_1=\lambda_2$ = 1).

Displacement mode shapes of functionally graded annular plate with mentioned supports are illustrated in Figs. 12-15.

5. Conclusions

The three-dimensional free vibrations of multi-directional graded circular and annular plates are analyzed by the state space based differential quadrature method, which solves dimensionless equations of motion analytically along thickness direction and numerically along radial direction of the plate. The natural frequencies and corresponding displacement mode shapes are obtained. The accuracy and convergence of the method are shown and it is illustrated that the method has proper accuracy and rapid converge. The numerical results are

compared with simpler cases presented in literature and the agreement is clear. The natural frequencies for circular plates with two different boundary conditions are presented. According to the numerical results, the natural frequencies increase when the circular or annular plate becomes thicker. This is observed by increasing thickness-to-outer radius ratios. Increasing the inner radius-to-outer radius ratio leads to an increase in the natural frequencies of annular plate. The influence of the graded indices on natural frequencies of the clamped circular plate is illustrated. It is shown that increasing the absolute value of along-radial graded index increases the natural frequencies but increasing through-thickness graded index decreases the natural frequencies. It is found that, plates having symmetric through-thickness graded indices have the same natural frequencies, because these plates are physically the same. According to these analyzes and parametric studies, a plate with acceptable variable material properties may be designed.

Nomenclature

a : Radius of circular plate

B_1, B_2 : The coefficients of the state variable formulation, give in Appendix

$\bar{B}_1, \bar{B}_2$: 3 × 3 non-dimensional coefficients of the state space formulation. They are function of R, only

$\left(\bar{B}_i\right)_1, \left(\bar{B}_i\right)_2$: 3N × 3N matrices obtained by applying the DQM on $\bar{B}_1$ and $\bar{B}_2$

B_i : $\begin{bmatrix} 0 & I \\ \left(\bar{B}_i\right)_1 & \left(\bar{B}_i\right)_2 \end{bmatrix}$

C_{ij} : Elastic stiffness components

C_{ij}^0 : The reference elastic stiffness components at the center of bottom plane of the plate, $z = 0$

$\bar{C}_{ij}^0$: Non-dimensional elastic stiffness components at the center of bottom plane, $z = 0$

E : Young's modulus

E^0 : The reference Young's modulus at the center of the bottom plane of the plate, $z = 0$

$f(R)$: A one-variable function whose derivative is developed based on its values in DQM

$f(R_i)$: $f(R)$ computed at discrete point i

h : Thickness of circular plate

$I_{3\times3}$: Identity matrix of dimension 3

i : $\sqrt{-1}$

$M(R_i)$: $\prod_{\substack{j=1 \\ i\neq j}}^{N}\left(R_i - R_j\right)$

m : The number of circumferential waves

N : The number of discrete points in DQM

R, Z : Non-dimensional radial and thickness variables

r, θ, z : Polar coordinates

t : Time variable

u_r, u_θ : In-plane displacements along the radial and circumferential directions of plate

u_z : Out-of-plane displacement along the thickness direction of the plate

U_R, U_θ, U_Z : Non-dimensional displacements along the radial, circumferential, and thickness directions

$W_{ij}^{(n)}$: nth-order weighting coefficient components

$[W_{ij}^{(n)}]$: Weighting coefficient matrix in DQM

$\gamma_{r\theta}$: In-plane shear strain

$\gamma_{\theta z}$, γ_{rz} : Out-of-plane shear strains

ε_r, ε_θ : In-plane normal strains along the radial and circumferential directions

ε_z : Out-of-plane normal strain along the thickness direction of the plate

λ_1 : Material property graded index along the thickness direction

λ_2 : Material property graded index along the radial direction

ν : Poisson's ratio

Π, Γ : State variables, $\Pi = \begin{bmatrix} u_r & u_\theta & u_z \end{bmatrix}^T$,

$$\Gamma = \begin{bmatrix} \frac{\partial u_r}{\partial z} & \frac{\partial u_\theta}{\partial z} & \frac{\partial u_z}{\partial z} \end{bmatrix}^T$$

$\bar{\Pi}, \bar{\Gamma}$: Non-dimensional state variables,

$$\bar{\Pi} = \begin{bmatrix} U_R & U_\theta & U_Z \end{bmatrix}^T,$$

$$\bar{\Gamma} = \begin{bmatrix} \frac{\partial U_R}{\partial Z} & \frac{\partial U_\theta}{\partial Z} & \frac{\partial U_Z}{\partial Z} \end{bmatrix}^T$$

$\bar{\Pi}_i, \bar{\Gamma}_i$: Discretized non-dimensional state variables,

$$\bar{\Pi}_i = \begin{bmatrix} \left[U_{R1}, U_{R2}, ..., U_{RN}\right]^T \\ \left[U_{\theta 1}, U_{\theta 2}, ..., U_{\theta N}\right]^T \\ \left[U_{Z1}, U_{Z2}, ..., U_{ZN}\right]^T \end{bmatrix},$$

$$\bar{\Gamma}_i = \begin{bmatrix} \left[\left(\frac{\partial U_R}{\partial Z}\right)_1, \left(\frac{\partial U_R}{\partial Z}\right)_2, ..., \left(\frac{\partial U_R}{\partial Z}\right)_N\right]^T \\ \left[\left(\frac{\partial U_\theta}{\partial Z}\right)_1, \left(\frac{\partial U_\theta}{\partial Z}\right)_2, ..., \left(\frac{\partial U_\theta}{\partial Z}\right)_N\right]^T \\ \left[\left(\frac{\partial U_Z}{\partial Z}\right)_1, \left(\frac{\partial U_Z}{\partial Z}\right)_2, ..., \left(\frac{\partial U_Z}{\partial Z}\right)_N\right]^T \end{bmatrix}$$

$\bar{\Pi}_i'(0)$: $\begin{bmatrix} \left[U_{R2}(0), ..., U_{R(N-1)}(0)\right]^T \\ \left[U_{\theta 2}(0), ..., U_{\theta(N-1)}(0)\right]^T \\ \left[U_{Z2}(0), ..., U_{Z(N-1)}(0)\right]^T \end{bmatrix}$

$\bar{\Pi}_i'(1)$: $\begin{bmatrix} \left[U_{R2}(1), ..., U_{R(N-1)}(1)\right]^T \\ \left[U_{\theta 2}(1), ..., U_{\theta(N-1)}(1)\right]^T \\ \left[U_{Z2}(1), ..., U_{Z(N-1)}(1)\right]^T \end{bmatrix}$

ρ : Material density

ρ^0 : The reference material density at the center of bottom plane, $z = 0$

σ_r, σ_θ : In-plane normal stresses along the radial and circumferential directions of the plate

σ_z : Out-of-plane normal stress along the thickness direction of the plate
$\tau_{r\theta}$: In-plane shear stress
$\tau_{\theta z}$, τ_{rz} : Out of-plane shear stresses
Ω : Non-dimensional natural frequency
ω : Natural frequency

References

[1] T. Prakash and M. Ganapathi, Asymmetric flexural vibration and thermoelastic stability of FGM circular plates using finite element method, *Composites Part B-Engineering*, 37 (2006) 642-649.

[2] E. Efraim and M. Eisenberger, Exact vibration analysis of variable thickness thick annular isotropic and FGM plates, *Sound and Vibration*, 299 (2007) 720-738.

[3] C. Y. Dong, Three-dimensional free vibration analysis of functionally graded annular plates using the Chebyshev-Ritz method, *Materials and Design*, 29 (2008) 1518-1525.

[4] A. Allahverdizadeh, M. H. Naei and M. Nikkhah Bahrami, Nonlinear free and forced vibration analysis of thin circular functionally graded plates, *Sound and Vibration*, 310 (2008) 966-984.

[5] G. J. Nie and Z. Zhong, Vibration analysis of functionally graded annular sectorial plates with simply supported radial edges, *Composite Structures*, 84 (2008) 167-176.

[6] A. Rastgoo, Analytical investigation on axisymmetric free vibrations of moderately thick circular functionally graded plate integrated with piezoelectric layers, *Journal of Mechanical Science and Technology*, 22 (2008) 1058-1072.

[7] P. Malekzadeh, M. M. Atashi and G. Karami, In-plane free vibration of functionally graded circular arches with temperature-dependent properties under thermal environment, *Sound and Vibration*, 326 (2009) 837-851.

[8] F. Ebrahimi, Geometrically nonlinear vibration analysis of piezoelectrically actuated FGM plate with an initial large deformation, *Journal of Mechanical Science and Technology*, 23 (2009) 2107-2124.

[9] A. Ghorbanpour Arani, A. Loghman, A. R. Shajari and S. Amir, Semi-analytical solution of magneto-thermo-elastic stresses for functionally graded variable thickness rotating disks, *Journal of Mechanical Science and Technology*, 24 (2010) 2107-2117.

[10] M. Malekzadeh, A. Shahpari and H. R. Ziaee, Three-dimensional free vibration of thick functionally graded annular plates in thermal environment, *Sound and Vibration*, 329 (2010) 425-442.

[11] S. Hosseini Hashemi, M. Fadaee and M. Eshaghi, A novel approach for in-plane/out-of-plane frequency analysis of functionally graded circular/annular plates, *International Journal of Mechanical Sciences*, 52 (2010) 1025-1035.

[12] A. Shahrjerdi, F. Mustapha, M. Bayat and D. L. A. Majid, Free vibration analysis of solar functionally graded plates with temperaturedependent material properties using second order shear deformation theory, *Journal of Mechanical Science and Technology*, 25 (2011) 2195-2209.

[13] Y. X. Hao, W. Zhang, J. Yang and S. Y. Li, nonlinear dynamic response of a simply supported rectangular functionally graded material plate under the time-dependent thermalmechanical loads, *Journal of Mechanical Science and Technology*, 25 (2011) 1637-1646.

[14] L. F. Qian and R. C. Batra, Design of bidirectional functionally graded plate for optimal natural frequencies, *Sound and Vibration*, 280 (2005) 415-424.

[15] G. Nie and Z. Zhong, Axisymmetric bending of two-directional functionally graded circular and annular plates, *Acta Mechanica Solida Sinica*, 20 (2007) 289-295.

[16] C. F. Lu, W. Q. Chen, R. Q. Xu and C. W. Lim, Semi-analytical elasticity solutions for bi-directional functionally graded beams, *International Journal of Solids and Structures*, 45 (2008) 258-275.

[17] M. Nemat-alla, K. I. E. Ahmed and I. Hassab-alla, Elastic-plastic analysis of two-directional functionally graded materials under thermal loading, *International Journal of Solids and Structures*, 46 (2009) 2774-2786.

[18] C. F. Lu, C. W. Lim and W. Q. Chen, Semi-analytical analysis for multi-directional functionally graded plates: 3-D elasticity solutions, *International Journal of Numerical Methods in Engineering*, 79 (2009) 25-44.

[19] G. J. Nie and Z. Zhong, Dynamic analysis of multi-directional functionally graded annular plates, *Applied Mathematical Modelling*, 34 (2010) 608-616.

[20] B. Sobhani Aragh, H. Hedayati, E. Borzabadi Farahani and M. Hedayati, Anovel 2-D six-parameter power-law distribution for free vibration and vibrational displacements of two-dimensional functionally graded fiber-reinforced curved panels, *European Journal of Mechanics A-Solids*, 30 (2011) 865-883.

[21] K. M. Liew and F. L. Liu, Differential quadrature method for vibration analysis of shear deformable annular sector plates, *Sound and Vibration*, 230 (2000) 335-356.

[22] S. Kitipornchai, J. Yang and K. M. Liew, Semi-analytical solution for nonlinear vibration of laminated FGM plates with geometric imperfections, *International Journal of Solids and Structures*, 41 (2004) 2235-2257.

[23] D. Redekop, Three-dimensional free vibration analysis of inhomogeneous thick orthotropic shells of revolution using differential quadrature, *Sound and Vibration*, 291 (2006) 1029-1040.

[24] K. Kang, Vibration analysis of thin-walled curved beams using DQM, *Journal of Mechanical Science and Technology*, 21 (2007) 1207-1217.

[25] A. Krowiak, Methods based on the differential quadrature in vibration analysis of plates, *Journal of Theoretical and Applied Mechanics*, 46 (2008) 123-139.

[26] F. Tornabene, Free vibration analysis of functionally graded conical, cylindrical shell and annular plate structures with a four-parameter power-law distribution, *Computer Method in Applied Mechanics and Engineering*, 198 (2009) 2911-2935.

[27] F. Tornabene, E. Viola and D. J. Inman, 2-D differential quadrature solution for vibration analysis of functionally graded conical, cylindrical shell and annular plate structures, *Sound and Vibration*, 328 (2009) 259-290.
[28] S. Hosseini Hashemi, H. Rokni damavandi Taher and H. Akhavan, Vibration analysis of radially FGM sectorial plates of variable thickness on elastic foundation, *Composite Structures*, 92 (2010) 1734-1743.
[29] W. Q. Chen, C. F. Lv and Z. G. Bian, Free vibration analysis of generally laminated beams via state-space-based differential quadrature, *Composite Structures*, 63 (2004) 417-425.
[30] G. J. Nie and Z. Zhong, Semi-analytical solution for three-dimensional vibration of functionally graded circular plates, *Computer Method in Applied Mechanics and Engineering*, 196 (2007) 4901-4910.
[31] L. Yang and S. Zhifei, Free vibration of a functionally graded piezoelectric beam via state-space based differential quadrature, *Composite Structures*, 87 (2009) 257-264.
[32] A. Jodaei, M. Jalal and M. H. Yas, Free vibration analysis of functionally graded annular plates by state-space based differential quadrature method and comparative modeling by ANN, *Composites Part B-Engineering*, 43 (2012) 340-353.
[33] F. Delale and F. Erdogan, The crack problem for a nonhomogeneous plane, *ASME Journal of Applied Mechanic*s, 50 (1983) 609-614.
[34] C. W. Bert and M. Malik, Differential quadrature method in computational mechanics: A review, *Applied Mechanics Reviews*, 49 (1996) 1-27.
[35] F. R. Gantmacher, *The Theory of Matrices*, Chelsea, New York, USA (1960).
[36] C. F. Liu and Y. T. Lee, Finite element analysis of three-dimensional vibrations of thick circular and annular plates, *Sound and Vibration*, 233 (2000) 63-80.

Appendix

The matrix B_1 is as follows:

$$B_1=\begin{bmatrix} b_{11}^1 & b_{12}^1 & b_{13}^1 \\ b_{21}^1 & b_{22}^1 & b_{23}^1 \\ b_{31}^1 & b_{32}^1 & b_{33}^1 \end{bmatrix}$$

where

$$b_{11}^1=-\frac{C_{11}^0}{C_{55}^0}\left(\frac{1}{r}\frac{\partial}{\partial r}+\frac{\partial^2}{\partial r^2}+\frac{\lambda_2}{a}\frac{\partial}{\partial r}\right)-\frac{C_{12}^0}{C_{55}^0}\frac{\lambda_2}{a}\frac{1}{r}+\frac{C_{22}^0}{C_{55}^0}\frac{1}{r^2}-\frac{C_{66}^0}{C_{55}^0}\frac{1}{r^2}\frac{\partial^2}{\partial\theta^2}+\frac{\rho^0}{C_{55}^0}\frac{\partial^2}{\partial t^2},$$

$$b_{12}^1=-\frac{C_{12}^0}{C_{55}^0}\left(\frac{1}{r}\frac{\partial^2}{\partial r\partial\theta}+\frac{\lambda_2}{a}\frac{1}{r}\frac{\partial}{\partial\theta}\right)+\frac{C_{22}^0}{C_{55}^0}\frac{1}{r^2}\frac{\partial}{\partial\theta}-\frac{C_{66}^0}{C_{55}^0}\left(\frac{1}{r}\frac{\partial^2}{\partial r\partial\theta}-\frac{1}{r^2}\frac{\partial}{\partial\theta}\right),$$

$$b_{13}^1=-\frac{\lambda_1}{h}\frac{\partial}{\partial r},$$

$$b_{21}^1=-\frac{C_{12}^0}{C_{44}^0}\frac{1}{r}\frac{\partial^2}{\partial r\partial\theta}-\frac{C_{22}^0}{C_{44}^0}\frac{1}{r^2}\frac{\partial}{\partial\theta}-\frac{C_{66}^0}{C_{44}^0}\left(\frac{1}{r^2}\frac{\partial}{\partial\theta}+\frac{1}{r}\frac{\partial^2}{\partial r\partial\theta}+\frac{\lambda_2}{a}\frac{1}{r}\frac{\partial}{\partial\theta}\right),$$

$$b_{22}^1=-\frac{C_{22}^0}{C_{44}^0}\frac{1}{r^2}\frac{\partial^2}{\partial\theta^2}+\frac{\rho^0}{C_{44}^0}\frac{\partial^2}{\partial t^2}-\frac{C_{66}^0}{C_{44}^0}\left(\frac{1}{r}\frac{\partial}{\partial r}+\frac{\partial^2}{\partial r^2}-\frac{\lambda_2}{a}\frac{1}{r}+\frac{\lambda_2}{a}\frac{\partial}{\partial r}-\frac{1}{r^2}\right),$$

$$b_{23}^1=-\frac{\lambda_1}{h}\frac{1}{r}\frac{\partial}{\partial\theta},$$

$$b_{31}^1=-\frac{C_{13}^0}{C_{33}^0}\frac{\lambda_1}{h}\frac{\partial}{\partial r}-\frac{C_{23}^0}{C_{33}^0}\frac{\lambda_1}{h}\frac{1}{r},$$

$$b_{32}^1=-\frac{C_{23}^0}{C_{33}^0}\frac{\lambda_1}{h}\frac{1}{r}\frac{\partial}{\partial\theta},$$

$$b_{33}^1=-\frac{C_{44}^0}{C_{33}^0}\frac{1}{r^2}\frac{\partial^2}{\partial\theta^2}-\frac{C_{55}^0}{C_{33}^0}\left(\frac{1}{r}\frac{\partial}{\partial r}+\frac{\partial^2}{\partial r^2}+\frac{\lambda_2}{a}\frac{\partial}{\partial r}\right)+\frac{\rho^0}{C_{33}^0}\frac{\partial^2}{\partial t^2}.$$

The matrix B_2 is as follows:

$$B_2=\begin{bmatrix} b_{11}^2 & b_{12}^2 & b_{13}^2 \\ b_{21}^2 & b_{22}^2 & b_{23}^2 \\ b_{31}^2 & b_{32}^2 & b_{33}^2 \end{bmatrix}$$

where

$$b_{11}^2=-\frac{\lambda_1}{h},$$

$$b_{12}^2=0,$$

$$b_{13}^2=-\frac{C_{13}^0}{C_{55}^0}\left(\frac{\partial}{\partial r}+\frac{1}{r}+\frac{\lambda_2}{a}\right)+\frac{C_{23}^0}{C_{55}^0}\frac{1}{r}-\frac{\partial}{\partial r},$$

$$b_{21}^2=0,$$

$$b_{22}^2=-\frac{\lambda_1}{h},$$

$$b_{23}^2=-\frac{C_{23}^0}{C_{44}^0}\frac{1}{r}\frac{\partial}{\partial\theta}-\frac{1}{r}\frac{\partial}{\partial\theta},$$

$$b_{31}^2=-\frac{C_{13}^0}{C_{33}^0}\frac{\partial}{\partial r}-\frac{C_{23}^0}{c_{33}^0}\frac{1}{r}-\frac{C_{55}^0}{C_{33}^0}\left(\frac{1}{r}+\frac{\partial}{\partial r}+\frac{\lambda_2}{a}\right),$$

$$b_{32}^2=-\frac{C_{23}^0}{C_{33}^0}\frac{1}{r}\frac{\partial}{\partial\theta}-\frac{C_{44}^0}{C_{33}^0}\frac{1}{r}\frac{\partial}{\partial\theta},$$

$$b_{33}^2=-\frac{\lambda_1}{h}.$$

Iman Davoodi Kermani received his B.Sc. degree in mechanical engineering in Shahid Bahonar University of Kerman, Kerman, Iran, in 2008. He received his M.Sc. degree in department of mechanical engineering of Isfahan University of Technology, Isfahan, Iran, in 2011. His research interests are vibration and stress analysis of plates and functionally graded materials (FGMs).

Mostafa Ghayour received his B.Sc. and M.Sc. degrees in Mechanical Engineering from University of Tehran, Tehran, Iran, in 1978. He received his Ph.D degree in Robotics from Isfahan University of Technology, Isfahan, Iran, in 1998. Now, he is Associate Professor of Mechanical Engineering on Robotics in Isfahan University of technology. His research interests include robotics, vibrations and control.

Hamid Reza Mirdamadi received his BSc in Civil Engineering, in 1986, MSc with honour, in Structural Engineering, in 1990, and Ph.D with honour, in Structural-Earthquake Engineering in 1999, all from Sharif University of Technology (SUT), Iran. Currently, he is an Assistant Professor at the Department of Mechanical Engineering, Isfahan University of Technology, Iran. His main research interests include smart structures (dynamics, vibrations, and controls), smart piezoelectric materials, micro/nano electromechanical systems (MEMS/NEMS), fluid-structure interaction, structural health monitoring (SHM), and structural system identification.